Optica Applicata, Vol. XIX, No. 3, 1989

Simulation of anticipated operation characteristics of designed constructions of broad-contact double-heterostructure (AlGa)As diode lasers. I. Threshold current*

W. Nakwaski

Institute of Physics, Technical University of Łódź, ul. Wólczańska 219, 93–005 Łódź, Poland.

The model of broad-contact double-heteostructure (AlGa)As diode laser is presented. It enables us to determine the anticipated threshold current of a designed laser structure.

1. Introduction

In a design of a diode laser structure of desired operation characteistics, the trial-and-error method is usually used. This method is the most expensive and the most time-consuming one.

A computer-aided micro-scale simulation of physical phenomena taking place within the laser crystal is a much better solution to this problem. Such a simulation is, however, very difficult, since then not only electrical, optical and thermal processes within a laser crystal but also their mutual interactions should be taken into account.To this end, a powerful computer is required and the solution is much time-consuming.

In the present work, a compromising solution is proposed. Physical phenomena are described with the aid of formulae which were derived in orginal works and include some material parameters. The latter have been determined by using the published experimental data.

The author does not regard the presented model as a finished, entirely formed work. Its present shape is only the first proposition although the author did his best in searching for the most reliable and recent literature data. The model should be modified when new, more correct data are published. If some experimental data (different from those known from literature) for materials used are available, they should be employed instead of literature ones.

Although the work deals with broad-contact lasers, the presented formulae may be to some extent useful also for modelling the behaviour of stripe-geometry lasers. This refers especially to all empirical formulae describing approximately the known experimental results.

---

* This work was carried out under the Polish Central Program for Fundamental Research CPBP 01.06., 6.04.

Schematic configuration of a diode laser, depicting some of structure parameters employed in the analysis, is shown in Fig. 1.

In the present part of the work, the gain threshold current and the leakage currents are considered. Two successive parts will deal with free-carrier absorption, quantum efficiencies and temperature effects. Some preliminary results have been recently presented in [1], whereas this paper reports the detailed results.

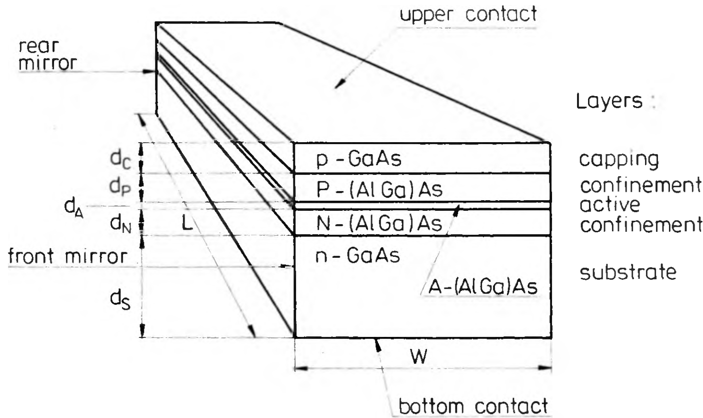

Fig. 1. Schematic configuration of a broad-contact double-heterostructure (AlGa)As diode laser

2. Threshold current density

Threshold current density of a diode laser reads as follows:

$$j_{TH} = j_{TH,G} + j_E + j_H \tag{1}$$

where $j_{TH,G}$ is the gain threshold current density, and j_E and j_H are the electron and the hole, respectively, leakage current densities.

3. Gain threshold current density

Gain threshold current density is given by the relation [2]

$$j_{TH,G} = \frac{d_A}{\eta_i} \frac{1\ \mu m}{} \left(\frac{g_{TH}}{\beta_s} + j_i \right) \tag{2}$$

where d_A is the active layer thickness, η_i – the internal quantum efficiency, g_{TH} – the threshold local gain, and β_s and j_i are the parameters which on the basis of [2]–[4] may be expressed for 250 K < T < 350 K in the following form:

$$\beta_s[\mathrm{cm/A}] = \begin{cases} 16.5 \times T^{-1.42} & \text{for } T < 300 \text{ K}, \\ 1.30 \times T^{-0.526} & \text{for } T > 300 \text{ K}, \end{cases} \tag{3}$$

$$j_i[\mathrm{A/cm^2}] = 2.16 \times T^{1.34}, \tag{4}$$

the exactness of the above formulae being not worse than 1.5%.

4. Threshold gain

The threshold local gain can be obtained from the following relation:

$$g_{TH} = (\alpha_{END} + \alpha_i)/\Gamma \tag{5}$$

where α_{END} and α_i are the end and the internal losses, respectively, and Γ is the confinement factor.

5. Confinement factor

The confinement factor may be expressed in the following form [5]:

$$\Gamma = D^2/(2 + D^2), \tag{6}$$

with

$$D = 2\pi(d_A/\lambda)\left[(n_{RA})^2 - (n_{RB})^2\right]^{1/2} \tag{7}$$

where λ is the radiation wavelength and n_{RA} and n_{RB} are the refractive indices of the active layer and the confinement layer materials, respectively.

6. Index of refraction

Based on the papers [6]–[9], the index of refraction in the $Al_xGa_{1-x}As$ material reads as follows:

$$n_R(x, T, n_F) = (3.590 - 0.710x + 0.091x^2 \\ \times [1 + (T - 297)4.9 \times 10^{-4}] - 1.2 \times 10^{-20} n_F \tag{8}$$

where x is the AlAs mole fraction and n_F is the free carrier concentration (in cm^{-3}).

7. Wavelength

Wavelength is usually determined with the aid of a simple approximate relation

$$\lambda\,[\mu m] = 1.2398/E_{G\Gamma}\ [eV] \tag{9}$$

where $E_{G\Gamma}$ is the direct energy gap, which – on the basis of papers [10]–[14] – may be written for $x_A \leq 0.45$ as

$$E_{G\Gamma}(x_A, n, p, T_A) = [1.519 - 5.405 \times 10^{-4}(1 + 0.6x_A)\,T_A^2/(T_A + 204\ K)] \\ \times (0.9375 + 0.8209x_A) - 1.6 \times 10^{-8}(n^{1/3} + p^{1/3}).\quad [eV]. \tag{10}$$

In the above relation, x_A is the AlAs mole fraction in the active layer material, T_A – the temperature of the active layer, and n and p are the electron and the hole concentrations, respectively, which should be substituted in cm^{-3}.

8. End losses

End losses may be expressed as

$$\alpha_{END} = (1/2L)\ln[1/(R_F R_R)] \tag{11}$$

where L is the length of the resonator, and R_F and R_R are the reflection coefficients from the front and the rear mirrors, respectively. The reflection coefficient R may be correlated with the refractive index n_R by means of the following well known relation:

$$R = [(n_R - 1)/(n_R + 1)]^2. \tag{12}$$

9. Internal losses

In the case of double-heterostructure lasers, internal losses may be expressed in form of the following sum:

$$\alpha_i = \Gamma\alpha_{FC} + (1-\Gamma)\alpha_{OUT} + \alpha_S + \alpha_C \tag{13}$$

where α_{FC} and α_{OUT} are the free-carrier losses in the active and the confinement layers, α_s – the scattering losses, and α_C are the coupling losses. Two first losses will be considered separately in the second part of the work.

10. Coupling losses

On the basis of Figure 1 published in paper [15], the coupling losses for one heterojunction may be obtained from the following relation

$$\alpha_C\,[\mathrm{cm}^{-1}] = \begin{cases} 120[130\exp(-4.87\, d_B/d_{B,MIN})^{-1}] & \text{for } d_B < d_{B,MIN} \\ 0 & \text{for } d_B > d_{B,MIN} \end{cases} \tag{14}$$

where d_B is the thickness (d_P or d_N) of the confinement layer adjacent to the considered heterojunction, and $d_{B,MIN}$ may be determined with the aid of the following expression:

$$d_{B,MIN}[\mu\mathrm{m}] = 0.3175\exp(-2.8\, d_A)\,[\mu\mathrm{m}])/(x_B - x_A), \tag{15}$$

x_B is the AlAs mole fraction in the confinement layers.

11. Scattering losses

A very thin ($\leqslant 0{,}2$ μm) active layer (c.f., Eq. (2)) is employed in order to achieve low threshold currents in DH diode lasers. The variations of threshold currents in these lasers are larger than in lasers with thicker active layers. They may be explained by the optical scattering losses due to nonplanar interfaces between the active layer and the confinement layers. Assuming that the optical losses are due to growth terraces

observed experimentally [16], the coefficient α_S connected with these losses may be written as [17]

$$\alpha_S = \frac{l_T N_T}{L} \frac{\gamma^2}{\beta(1+0.5\gamma d_A)} \frac{\varkappa^2}{[(n_{RA})^2 - (n_{RB})^2] k_0^2} \exp(\gamma d_A) \exp(-2\gamma^3 r_T / 3\beta^2) \tag{16}$$

where r_T and l_T are the radius of curvature of the bent section and the length of the riser section of the terrace, respectively (see Fig. 2), N_T is the number of the growth terraces in the cavity, γ is the propagation constant which may be determined from the following equation:

$$\gamma = \varkappa \tan(\varkappa d_A/2), \tag{17}$$

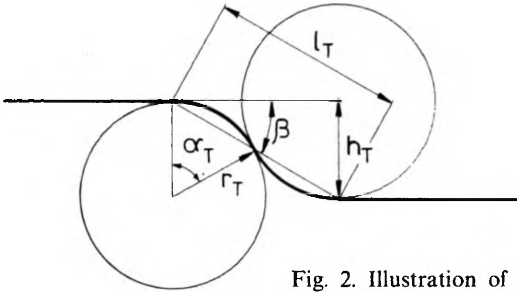

Fig. 2. Illustration of a derivation of the formula (26)

and the remaining parameters may be calculated from the relations:

$$\beta^2 = \gamma^2 + (n_{RB})^2 k_0^2, \tag{18}$$

$$\varkappa^2 = (n_{RA})^2 - \beta^2, \tag{19}$$

$$k_0 = 2\pi/\lambda. \tag{20}$$

For thin active layers fulfilling the condition

$$d_A \leqslant 0.07\,\lambda/(x_B - x_A)^{1/2}, \tag{21}$$

we may use the approximate solution [18]

$$\gamma = 0.5\,\varkappa^2 d_A, \tag{22}$$

then β approaches the value

$$\beta = k_0 n_B, \tag{23}$$

and $\varkappa$ becomes equal to

$$\varkappa = [(n_{RA})^2 - (n_{RA})^2]^{1/2} k_0. \tag{24}$$

If the condition (21) is not fulfilled, we search for β using the relation [19]

$$\tan\{[n_{RA})^2 k_0^2 - \beta^2]^{1/2} (d_A/2)\} = [\beta^2 - (n_{RB})^2 k_0^2]^{1/2} / [(n_{RA})^2 k_0^2 - \beta^2]^{1/2}, \tag{25}$$

being the modified version of Eq. (17). The calculations may for instance be performed by means of the falsi rule with the step $\Delta\beta = n_{RB} k_0/2$. Then γ and $\varkappa$ can be determined from Eqs. (17) and (18).

The radius of curvature of the bent section of the terrace may in turn be determined in a following way (Fig. 2):

$$\sin\beta_T = h_T/l_T = \sin(\alpha_T/2) = l_T/4r, \tag{26}$$

what gives a final result in a form [16]

$$r_T = (l_T/2)^2/h_T. \tag{26a}$$

12. Leakage current densities

The electron j_E and the hole j_H leakage current densities across the heterojunctions into the P-(AlGa)As layer and into the N-(AlGa)As layer, respectively, may be expressed in the following way [20], [21]:

$$j_E = \frac{eD_E N_P}{L_E \tanh(d_P/L_E)}, \tag{27}$$

$$j_H = \frac{eD_H P_N}{L_H \tanh(d_N/L_H)}. \tag{28}$$

In Equations (27) and (28), D_E and D_H are respectively the electron diffusion coefficient in the P-type confinement layer and the hole diffusion coefficient in the analogous N-type layer, whereas L_E and L_H are the electron diffusion length in the P-type layer and the hole diffusion length in the N-type layer; N_P is the electron concentration at the edge of the P-type layer adjacent to the active layer and P_N is the hole concentration at the analogous edge of the N-type layer.

13. Electron and hole concentrations at the edges of the confining layers

Electron concentraction at the edge of the P-(AlGa)As layer (the edge adjacent to the active layer) may be expressed as

$$N_P = N_{CP}\exp[-(E_{CP}-F_{EP})/k_B T] \tag{29}$$

where N_{CP} is the conduction band effective density of states, E_{CP} – the conduction band edge, and F_{EP} – the electron quasi-Fermi level, all in the P-type material; k_B is the Boltzmann's constant.

The analogous formula for the hole concentration P_N at the analogous edge of the N-type layer reads as follows:

$$P_N = N_{VN}\exp[-(F_{HN}-E_{VN})/k_B T] \tag{30}$$

where N_{VN} is the valence band effective density of states, E_{VN} – the valence band edge and F_{HN} – the hole quasi-Fermi level, all in the N-type material.

14. Effective density of states

The effective density of states for all three conduction bands of the $Al_xGa_{1-x}As$ material may be calculated in the following way [22]:

$$N_C[\mathrm{cm}^{-3}] = 2.5\times10^{19}\{(m_{E\Gamma}/m_0)^{3/2}+(m_{EL}/m_0)^{3/2}\exp[(E_{G\Gamma}-E_{GL})/k_BT] + (m_{EX}/m_0)^{3/2}\exp[(E_{G\Gamma}-E_{GX})/k_BT]\}(T/300)^{3/2} \quad (31)$$

where m_0 is the free electron mass, $E_{G\Gamma}$, E_{GL} and E_{GX} are the Γ direct, the L indirect and the X indirect energy gaps, respectively, and m_E, m_{EL} and m_{EX} are the electron effective masses corresponding to the above conduction bands.

The analogous relation for the effective density of states for the valence band may be written as [23]

$$N_V[\mathrm{cm}^{-3}] = 2.5\times10^{19}(m_H/m_0)^{3/2}(T/300)^{3/2} \quad (32)$$

where m_H is the hole effective mass.

15. Indirect energy gaps

The compositional dependences of the indirect energy gaps of the $Al_xGa_{1-x}As$ material at room temperature may be given by [24]

$$E_{GL}[\mathrm{eV}] = 1.708+0.642x, \quad (33)$$

$$E_{GX}[\mathrm{eV}] = 1.900+0.125x+0.143x^2. \quad (34)$$

16. Effective masses

The electron effective masses for the three conduction bands of the $Al_xGa_{1-x}As$ material at room temperature may be obtained from the relations [24]:

$$m_{E\Gamma} = (0.067+0.083x)m_0, \quad (35)$$

$$m_{EL} = (0.55+0.12x)m_0, \quad (36)$$

$$m_{EX} = (0.85-0.07x)m_0. \quad (37)$$

The analogous hole effective mass for the valence band is taken as [24]

$$m_H = (0.48+0.31x)m_0. \quad (38)$$

17. Quasi-Fermi levels

From Figure 4 in paper [21] we may write

$$E_{CP}-F_{EP} = \Delta E_G+(F_{HA}-E_{VA})-(F_{HP}-E_{VP})-(F_{EA}-E_{CA}) \quad (39)$$

where F_{HA}, F_{HP} and F_{EA} are the hole quasi-Fermi levels in the active layer and in the P-type layer and the electron quasi-Fermi level in the active layer, respectively; E_{VA}, E_{VP} and E_{CA} are respectively the valence band edges in the active and in the P-type layers and the conduction band edge in the active layer ΔE_G is obtained from the relation

$$\Delta E_G = (E_{CP} - E_{VP}) - (E_{CA} - E_{VA}) = E_{GP} - E_{GA} \tag{40}$$

where E_{CP} and E_{CA} and the conduction band edges in the P-type layer and in the active layer, respectively, and E_{GP} and E_{GA} are the direct energy gaps in the above materials.

For the N-type material, the analogous formula may be written in the form [21]

$$F_{HN} - E_{VN} = \Delta E_G - (F_{EA} - E_{CA}) - (E_{CN} - F_{EN}) + (F_{HA} - E_{VA}) \tag{41}$$

where F_{EN} and E_{CN} are the electron quasi-Fermi level and the conduction band edge, both in the N-type material.

Let us introduce a function $F_{1/2}(\mu)$, being the Boltzmann approximation for the Fermi level, to the degenerate case and extended by JOYCE and DIXON [25]

$$F_{1/2}(\mu) = k_B T[\ln \mu + 3.53553 \times 10^{-1} \mu - 4.95009 \times 10^{-3} \mu^2 + 1.48386 \times 10^{-4} \mu^3 - 4.42563 \times 10^{-6} \mu^4. \tag{42}$$

Then the differences set in parantheses in Eqs. (39) and (41) may be obtained from the relations

$$F_{EA} - E_{CA} = F_{1/2}(n_A/N_{CA}), \tag{43}$$

$$F_{HA} - E_{VA} = -F_{1/2}(p_A/N_{VA}), \tag{44}$$

$$F_{HP} - E_{VP} = -F_{1/2}(P_P/N_{VP}), \tag{45}$$

$$F_{EN} - E_{CN} = F_{1/2}(N_N/N_{CN}) \tag{46}$$

where n_A, N_N, p_A and P_P are the electron concentrations in the active layer and in the N-type layer, and the hole concentrations in the active layer and in the P-type layer, respectively. N_{CA}, N_{CN}, N_{VA} and N_{VP} are the effective densities of states for the conduction bands in the active layer and the N-type layer and the effective densities of states for the valence bands in the active layer and in the P-type layer, respectively. They may be calculated bv means of the Eqs. (31) and (32).

18. Diffusion coefficients

The electron diffusion coefficient in the P-type layer and the hole diffusion coefficient in the N-type layer may be related to their mobilities by the Einstein relations:

$$D_E = \mu_E k_B T/e, \tag{47}$$

$$D_H = \mu_H k_B/e. \tag{48}$$

where μ_E and μ_H are the electron mobility in the P-type layer and the hole mobility in the N-type layer, respectively, and e is the unit charge. The composition dependence of the mobilities will be considered in the third part of the work.

19. Diffusion lengths

The formulae for the minority-carrier diffusion lengths in the $Al_xGa_{1-x}As$ material may, on the basis of papers [26]–[32] be written in the forms:

$$L_E[\mu m] = 8.8 f_L(x) \exp[-b_E(p)] [\mu_E(T)/\mu_E(300\,K)] (T/300)^{1.25x+1.29}, \tag{49}$$

$$L_H[\mu m] = 2.14 f_L(x) \exp[-b_H(n)] [\mu_H(T)/\mu_H(300\,K)] (T/300)^{1.25x+1.29} \tag{50}$$

where:

$$f_L(x) = 1 - a_L \exp(b_L x), \tag{51}$$

$$b_E(p) = 0.026 \exp[1.5 \log(p/10^{16})]. \tag{52}$$

$$b_H(n) = \begin{cases} 1.058 \times 10^{-3} \exp[2.76 \log(n/10^{16})] & \text{for } n < 4 \times 10^{18}\,cm^{-3} \\ 8.923 \times 10^{-3} \exp[1.933 \log(n/10^{16})] & \text{for } n \geqslant 4 \times 10^{18}\,cm^{-3} \end{cases} \tag{53}$$

and the a_L and b_L parameters are listed in the Table. In all the above expressions, carrier concentrations should be substituted in cm^{-3}. The exactness of the above approximations is not worse than 5.5% and 1.7% for L_E and L_H, respectively, for the concentration dependences, and 2.4% for the composition dependence.

Values of the parameters of the relation (51)

Parameter	$x < 0.32$	$x > 0.32$
a_L	1.377×10^{-2}	8.9×10^{-2}
b_L	1.078	4.93

20. Conclusions

The first part of the model broad-contact double-heterostructure (AlGa)As diode lasers was presented in this work. The model enables us to determine the anticipated threshold current of a desired laser structure from its structural parameters. The model may be used for optimization of the laser structure from the point of view of minimization of the threshold current density. In this case, however, the temperature dependence of all the processes of light generation and absorption becomes critical, so the self-consistent method of calculations, given in the third part of the work, should be used.

In the next two parts of the work, free-carrier absorption, quantum efficiencies and temperature effects will be analysed.

References

[1] Nakwaski W., Intern. Conf. *Trends in Quantum Electronics*, *TQE'88*, Bucharest 1988.
[2] Stern F., IEEE J. Quantum Electron. **QE-9** (1973), 290.
[3] Stern F., J. Appl. Phys. **47** (1976), 5382.
[4] Casey H. C., Jr, J. Appl. Phys. **49** (1978), 3684.
[5] Botez D., IEEE J. Quantum Electron. **QE 14** (1978), 230.
[6] Marple D. T. F., J. Appl. Phys. **35** (1964), 1241.
[7] Casey H. C., Jr, Sell D. D., Panish M. B., Appl. Phys. Lett. **24** (1974), 63.
[8] Cook D. D., Nash F. R., J. Appl. Phys. **46** (1975), 1660.
[9] Manning J., Olshansky R., Su C. B., IEEE J. Quantum Electron. **QE-19** (1983), 1525.
[10] Casey H. C., Jr, Panish M. B., *Heterostructure Lasers*, *Part B*: *Materials and Operating Characteristics*, Academic Press, New York 1978, p. 16, Table 5.3-1.
[11] Casey H. C., Jr, Panish M. B., *Heterostructure Lasers*, *Part A*: *Fundamental Principles*, Academic Press, New York 1978, p. 163.
[12] Casey H. C., Jr, Stern F., J. Appl. Phys. **47** (1976), 631.
[13] Thurmond C. D., J. Electrochem. Soc. **122** (1975), 1133.
[14] Vorobkalo F. M., Glinchuk K. D., Kovalenko V. F., Fiz. Tekh. Poluprovod. **9** (1975), 998 (in Russian).
[15] Casey H. C., Jr, Panish M. B., J. Appl. Phys. **46** (1975), 1393.
[16] Shima K., Segi K., Imai H., Fujiwara T., Takusagawa M., Appl. Phys. Lett. **37** (1980), 341.
[17] Nash F. R., Wagner W. R., Brown R. L., J. Appl. Phys. **47** (1976), 3992.
[18] Dumke W. P., IEEE J. Quantum Electron. **QE 11** (1975), 400.
[19] Marcuse D., *Light Transmission Optics*, van Nostrand Reinhold, New York 1972, Chapter 8.3.
[20] Reference[11], p. 249.
[21] Casey H. C., Jr, J. Appl. Phys. **49** (1978), 3684.
[22] Reference [11], p. 203.
[23] Reference [11], p. 206.
[24] Reference [11], p. 194.
[25] Joyce W. B., Dixon R. W., Appl. Phys. Lett. **31** (1977), 354.
[26] Anthony P. J., Pawlik J. R., Swaminathan V., Tsang W. T., IEEE J. Quantum Electron. **QE-19** (1983), 1030.
[27] Garbuzov D. N., [In] *Semiconductor Optoelectronics,* [Ed.] M.A. Herman, PWN, Warszawa 1980, p. 305.
[28] Garbuzov D. N., Khalfin V. B., Trukan M. K., Agafonov V. G., Abdullaev A., Fiz. Tekh. Poluprovod. **12** (1978), 1368 (in Russian).
[29] 't Hooft G. W., van Opdorp C., Appl. Phys. Lett. **42** (1983), 813.
[30] Casey H. C., Jr, Miller B. I., Pinkas E., J. Appl. Phys. **44** (1973), 1281.
[31] Rogulin V. Yu, Filler A.C., Shilenskii A. A., Fiz. Tekh. Poluprovod. **7** (1973), 1828 (in Russian).
[32] Kawakami T., Sogiyama K., Jpn. J. Appl. Phys. **12** (1973), 151.

Received March 30, 1989
in revised form May 16, 1989

Имитация предусматриваемых эксплуатационных характеристик ширококонтактных лазерных диодов (AlGa)As с двойной гетероструктурой. I. Пороговый ток

В настоящей работе представлена модель ширококонтактного лазерного диода (AlGa)As с двойной гетероструктурой. Эта модель делает возможным предусмотрение порогового тока проектированной лазерной структуры.